Semiconductor Physics, Quantum Electronics & Optoelectronics, 2012. V. 15, N 3. P. 204-208.

PACS 42.79.Dj, 78.35.+c

Resonance scattering and absorption of light by finite two-period gratings of circular silver nanowires

D.M. Natarov[1], R. Sauleau[2], A.I. Nosich[1]
[1]*Institute of Radio-Physics and Electronics, NAS of Ukraine,*
12, Proskury str. 61085 Kharkiv, Ukraine
E-mail: den.natarov@gmail.com
[2]*IETR, University of Rennes 1, Campus Beaulieu, bat 11-D, 35042 Rennes Cedex, France*
E-mail: ronan.sauleau@univ-rennes1.fr

Abstract. We consider the two-dimensional scattering of the H-polarized electromagnetic plane waves of the visible range by three types of gratings made of periodically arranged circular cylindrical sub-wavelength wires. Using the field expansions in local coordinates and addition theorems for cylindrical functions, we obtain a block-type matrix equation for the field expansion coefficients. This equation is of the Fredholm second-kind form that guarantees convergence of numerical solution. The scattering and absorption cross-sections and the near-field patterns are computed. The interplay of plasmon and grating-type resonances is studied for two and three-layer gratings of identical periods, stacked two-period gratings, and in-line two-period gratings made of nano-diameter silver wires.

Keywords: plasmon resonance, grating resonance, finite grating, nanowire, scattering, absorption, cross-section.

Manuscript received 08.05.12; revised version received 08.06.12; accepted for publication 14.06.12; published online 25.09.12.

1. Introduction

Two fundamental effects are known to influence the scattering of light by periodically structured metal scatterers. On the one hand, surface-plasmon resonances are observed for sub-wavelength noble-metal particles and wires in the mid-infrared and optical bands [1, 2]. Nanosize objects can exhibit resonance behavior at certain frequencies for which the object permittivity is negative. This results in powerful enhancement of scattered and absorbed light that is used in the design of optical antennas and biochemical sensors for advanced applications. In the leading terms, the plasmon resonance wavelength depends on the object shape but not on its dimensions.

On the other hand, periodically structured scatterers, or finite and infinite gratings, arrays or chains of particles and holes in metallic screens (in 3-D) or wires and slots (in 2-D), are attracting large attention of researchers in today nano-optics [3-6]. This is caused by the effects of extraordinarily large reflection, transmission, emission, and near-field enhancement that have been found in the scattering of light by periodic scatterers. Recently, it has been discovered that these phenomena are explained by the existence of the so-called grating resonances or poles of the field function [4-6] (a.k.a. geometrical, lattice and Bragg resonances). Their wavelengths lay near the Rayleigh wavelengths [7], i.e. near to period being a multiple of the wavelength, if all elementary scatterers of a grating are excited in the same phase, and their size is a fraction of the period. In the wave scattering by infinite gratings, they lead to almost total reflection of the incident field by a sparse thin-dielectric-wire grating in narrow wavelength bands [3, 5].

The goal of our paper is extension of this study to more complicated periodically structured silver-wire configurations where both plasmon and grating resonances are present.

2. Scattering problem and its numerical solution

Consider finite collections of M parallel wires illuminated by an H-polarized plane wave shown in

Fig. 1. The wires are assumed to be infinite circular cylinders, each having the radius a and complex relative dielectric permittivity ε. For a 2-D problem, one has to find a scalar function $H_z(\vec{r})$ that is the scattered magnetic-field z-component.

This function has to satisfy the Helmholtz equation with corresponding wavenumbers inside and outside the cylinders, the tangential field components continuity conditions, the radiation condition, and the condition of the local power finiteness. The full-wave numerical solution can be obtained similarly to [7, 8], by expanding the field function in terms of the azimuth exponents in the local polar coordinates, using addition theorems for cylindrical functions and applying the boundary conditions on the surface of each of M wires. This leads to an infinite $M \times M$ block-type matrix equation where each block is infinite. Still a close inspection shows that the matrix equations used in the mentioned above papers did not provide guaranteed convergence of solutions. Here, the convergence is understood in mathematical sense, as a possibility of minimizing the error of computations by solving progressively larger matrices. We fix this defect by re-scaling the unknown coefficients as explained in [6].

The obtained in such a way matrix equation is a block-type Fredholm second kind operator equation. In this case, the convergence of solution, after truncation of each block to finite order N, to an exact one if $N \to \infty$, is guaranteed by the Fredholm theorems. The results presented below were computed with $N = 4 \ldots 5$; this provided 3 correct digits in the far-field characteristics of the sparse gratings of silver wires with radii $a \leq 75$ nm and periods $p \geq 200$ nm. Note that denser gratings may need larger values of N to achieve the same accuracy.

We have considered three sparse ($p - 2a > 2a$) configurations of finite number of sub-wavelength silver nanowires: two and three-layer gratings of the same periods, stacked two-period gratings, and in-line two-period gratings (Fig. 1). Dense configurations are also interesting objects, however they deserve a separate study. To characterize the optical properties of considered discrete scatterers, we have used the wavelength dependences of the total scattering (TSCS) and the absorption (ACS) cross-sections and calculated the field patterns in the near zone. In Figs 2 to 6, the wavelength varies from 300 up to 500 nm, and the complex-valued dielectric function of silver has been borrowed from the classical paper of Johnson and Christy.

3. Optical response of two- and three-layer gratings

N-layer gratings are interesting structures for research, because they are periodic along two axes and can be considered as finite-size photonic or plasmonic crystals. How this structuring influences the grating and plasmon resonances is a question that needs clarification. Presented in Fig. 2 are per-wire TSCS and ACS as functions of the wavelength for the H-wave normal incidence on the gratings of two and three chains of 100 nanowires with radii a = 70 nm, with periods along the x-axis p_x = 360 nm and along the y-axis $p_y = 5a$. As known, the plasmon-resonance peak for a single silver nanowire in free space is near 350 nm, so both periods are in the vicinity of this value. As one can see, the resonant peaks of the averaged per-wire cross-sections are higher for two-layer grating. This can be understood as a result of shadowing of the lower layers by the upper (better illuminated) ones. The TSCS wavelength dependences have several local maxima in the vicinity of 350 nm, and in the case of the two-layer grating there is one resonance at 350–360 nm wavelengths, but in the case of the three-layer grating there are two low-quality resonances in the same range.

At the 383 and 394 nm wavelengths, one can see the highest resonances for the two- and three-layer gratings, respectively (see Fig. 3). Note that the ACS dependences show the peak values at the same wavelengths where TSCS dependences have their minima.

Presented in Fig. 3 are near-field amplitude patterns for the central part of the two- and three-layer gratings in the main resonances. The visualized part of the grating includes 11 central wires from each layer. One can see that the most intensive H-field maxima are located at the illuminated side of the upper-layer wires for the two-layer grating, and between the layers for the three-layer grating. Besides, one can see a standing wave above the illuminated side for each grating.

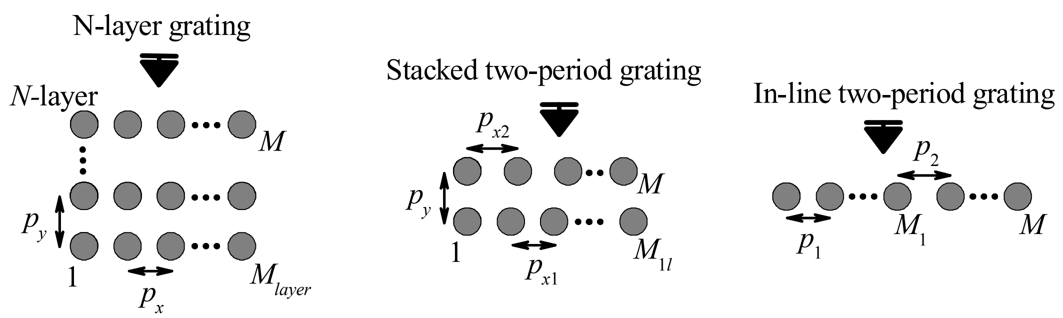

Fig. 1. Scattering problem geometries and notations.

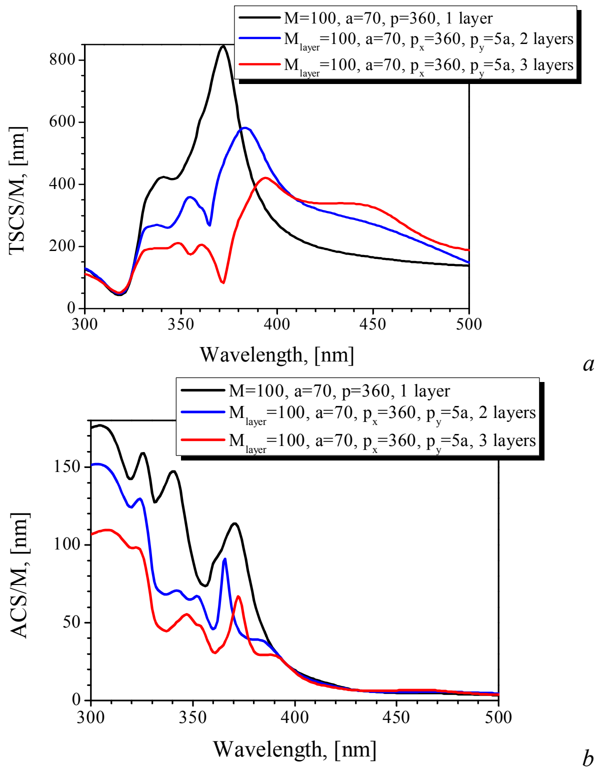

Fig. 2. Normalized per number of wires TSCS (a) and ACS (b) as functions of the wavelength for the H-wave normal incidence on the 1-, 2- and 3-layer gratings of identical silver wires.

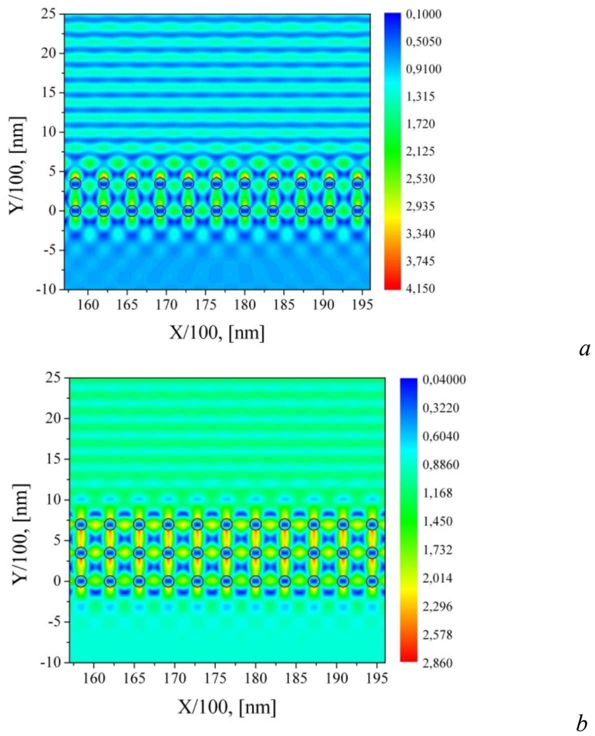

Fig. 3. Near-field amplitude patterns of the central parts of the two- and three-layer gratings from Fig. 2 in the TSCS maxima at the wavelengths 383 (a) and 394 nm (b). The incident plane wave comes from the upper half-space normally to the grating.

4. Optical response of two-period stacked and in-line gratings

Two-period linear gratings that consist of two chains or arms with different periods are interesting for applications because of existence of two different grating resonances, in addition to the plasmon resonance of each individual wire. This feature can be useful for electromagnetic engineering of the novel wideband absorbers for solar cells. Our analysis of such gratings have shown that it is indeed possible to combine the resonances and enhance the per-wire TSCS and ACS, if the wire radius is 50 nm or larger and their number is at least 100.

Presented in Fig. 4 are per-wire TSCS and ACS as functions of wavelength for the normal incidence of the H-wave on the stacked and in-line double-periodic gratings of silver nanowires with radii a = 70 nm and periods p_1 = 360 nm (180 or 179 wires) and p_2 = 450 nm (100 wires); the distance between the layers in the stacked grating is 210 nm. One can see that the cross-sections for the in-line configuration have more intensive and sharper resonances of both types, apparently because such a configuration has no part shaded by other wires. The TSCS reaches its maximum value at 374 and 372 nm for the stacked and in-line two-period gratings, respectively. This resonance is associated with the smaller period and, in part, with the plasmon resonance of each wire. The other grating resonance in the vicinity of the 450 nm wavelength (the larger period value) has low intensity, especially for ACS because the bulk losses in silver are smaller there.

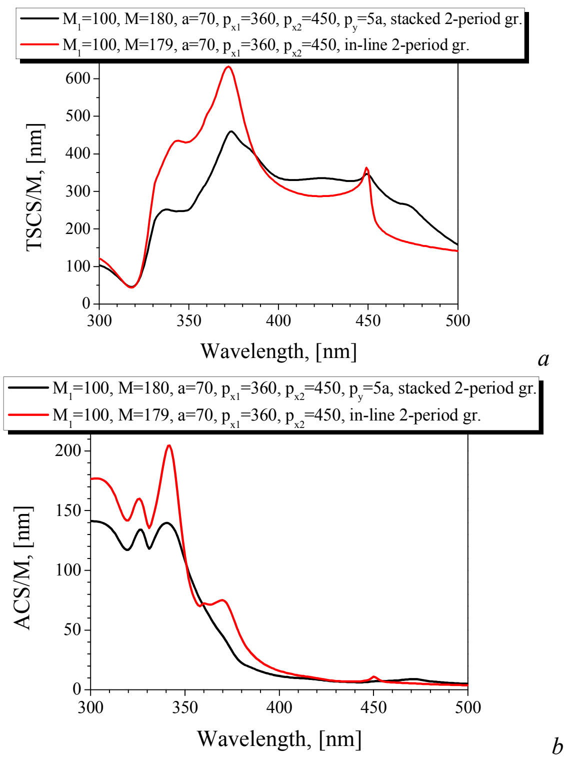

Fig. 4. Normalized TSCS (a) and ACS (b) as functions of the wavelength for the H-wave normally incident on the stacked and in-line two-period gratings of identical silver nanowires.

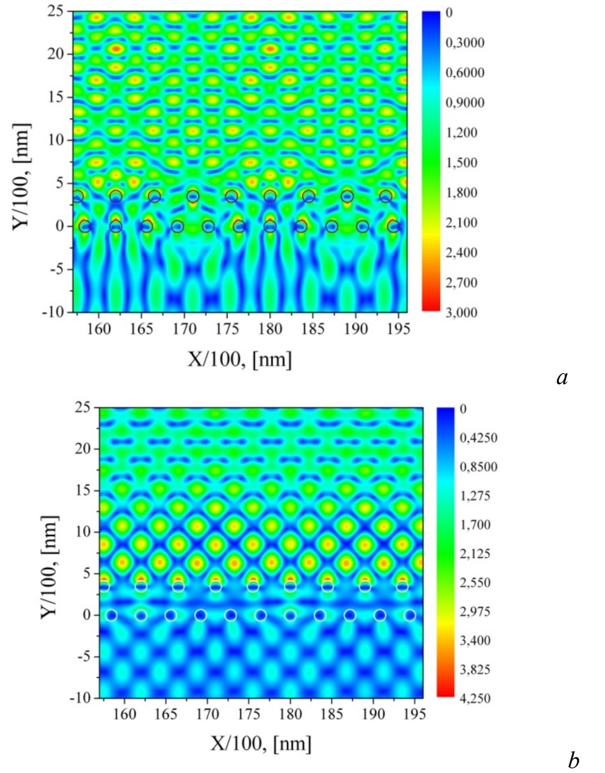

Fig. 5. Near-field amplitude patterns of the central parts of the stacked two-period grating from Fig. 4 in the grating resonances at the wavelengths 374 (a) and 449 nm (b). The incident plane wave comes from the upper half-space normally to the grating.

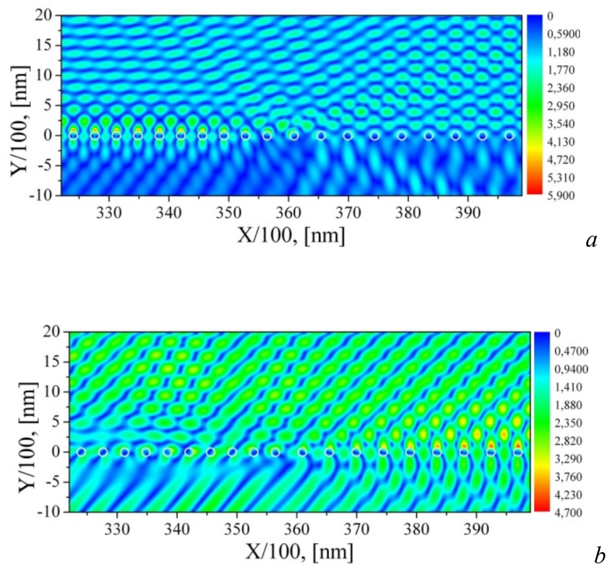

Fig. 6. Near-field amplitude patterns of the central parts of the in-line two-period grating from Fig. 4 in the grating resonances at the wavelengths 372 (a) and 449 nm (b). The incident plane wave comes from the upper half-space normally to the grating.

Presented in Figs. 5 and 6 are the near-field amplitude patterns for the central parts of the stacked and in-line two-period gratings, respectively, in the grating resonances. In Fig. 5, we show the near-field patterns at 374 and 449 nm in the grating resonances associated with the smaller and larger periods, respectively. Note that in the second case the field pattern demonstrates that the top grating (tuned into resonance) efficiently screens the bottom grating, which remains in the deep shadow. In Fig. 6, we show near-field patterns at 372 and 449 nm in the grating resonances for the smaller and larger periods of the in-line grating. In each case, the standing waves are formed along the x and y axes, however only near the arm of the grating that is tuned to the resonance.

5. Conclusions

We have presented results of accurate calculations of the scattering and absorption spectra for several periodically structured configurations made of silver nanowires, in the visible range. They demonstrate co-existence of plasmon resonances related to each silver wire and several grating-type resonances in structures with more than one period. At the wavelength of each grating resonance, the scattering and absorption demonstrate maxima. Visualization of in-resonance near fields shows that the contribution to these maxima comes from the corresponding sub-gratings whose period is tuned to the incoming wavelength. Presented results can be useful for the modelling of optical response of "photonic-plasmonic molecules" and for engineering the novel wideband absorbers for solar cells.

Acknowledgments

This work has been partially supported by the National Academy of Sciences of Ukraine via the State Target Program "Nanotechnologies and Nanomaterials" and the European Science Foundation via the Research Networking Programme "Newfocus".

References

1. V. Giannini and J.A. Sànchez-Gil, Calculations of light scattering from isolated and interacting metallic nanowires of arbitrary cross-section by means of Green's theorem surface integral equations in parametric form // *J. Opt. Soc. Am. A*, **24**(9), p. 241-248 (2007).
2. D.R. Fredkin, I. Mayergoyz, Resonant behavior of dielectric objects (electrostatic resonances) // *Phys. Rev. Lett.* **91**, p. 3902-3905 (2003).
3. M. Laroche, S. Albaladejo, R. Gomez-Medina, and J.J. Saenz, Tuning the optical response of nanocylinder arrays: an analytical study // *Phys. Rev. B*, **74**(9), p. 245422-10 (2006).

4. F.J.G. Garcia de Abajo, Colloquium: Light scattering by particle and hole arrays // *Rev. Mod. Phys.* **79**(4), p. 1267-1289 (2007).
5. V.O. Byelobrov, J. Ctyroky, T.M. Benson, et al., Low-threshold lasing eigenmodes of an infinite periodic chain of quantum wires // *Opt. Lett.* **35**(21), p. 3634-3636 (2010).
6. D.M. Natarov, V.O. Byelobrov, R. Sauleau, T.M. Benson, and A.I. Nosich, Periodicity-induced effects in the scattering and absorption of light by infinite and finite gratings of circular silver nanowires // *Opt. Express*, **19**(22), p. 22176-22190 (2011).
7. H.A. Ragheb, M. Hamid, Scattering by N parallel conducting circular cylinders // *Int. J. Electronics*, **59**(4), p. 407-421 (1985).
8. D. Felbacq, G. Tayeb, and D. Maystre, Scattering by a random set of parallel cylinders // *J. Opt. Soc. Am. A*, **11**(9), p. 2526-2538 (1994).